

SUPPLEMENTARY MATERIAL FOR

Biliverdin Chiral Derivatives as Chiroptical Switches for pH and Metal Cation Sensing

Simone Ghidinelli¹, Sergio Abbate^{1,2}, Giuseppe Mazzeo¹, Stefan E. Boiadjev³, David A. Lightner⁴,
Giovanna Longhi^{1,2}

¹Università di Brescia, Dipartimento di Medicina Molecolare e Traslazionale, Viale Europa 11,
25123 Brescia (Italy)

²Istituto Nazionale di Ottica (INO), C.N.R., Research Unit of Brescia, via Branze 45, 25123 Brescia
(Italy)

³Regional Health Inspectorate, 7 Prince Al. Battenberg I Str., 5800 Pleven (Bulgaria)

⁴Chemistry Department, University of Nevada, Reno, NV, 89557 (USA)

LIST OF FIGURES AND ITEMS

Figure SI-1. ECD spectra of **1** and **2** as a function of temperature.

Figure SI-2. Optimized 3D-structures of the most populated conformers of **1**.

Figure SI-3. Calculated IR and VCD spectra of the most populated conformers of **1**.

Figure SI-4. Optimized 3D-structures of the most populated conformers of **2**.

Figure SI-5. Calculated IR and VCD spectra of the most populated conformers of **2**.

Figure SI-6. Experimental UV and ECD spectra of **1** in methanol solution and after addition of HCl.

Figure SI-7. Experimental UV and ECD spectra of **2** in methanol and DMSO solution after addition
of NaOH.

Figure SI-8. Experimental UV and ECD spectra during the neutralization of basified methanol and
basified DMSO solutions of **2**.

Table SI-1. Boltzmann population factors for the main conformers in the neutral and protonated
condition for compound **1**.

Table SI-2. Boltzmann population factors for the main conformers in the neutral and deprotonated
condition for compound **2**.

Figure SI-9. Experimental ECD and UV spectra of 8,12-bis[(1*S*)-methylpropyl]mesobiliverdin-
XIII α , 8,12-bis[3-acetoxy-(1*S*)-methylpropyl]mesobiliverdin-XIII α , and **6** with addition of HCl or
NaOH.

Figure SI-10. Superposed DFT-calculated structures of 1*P* conformer of **1** and **2** in the neutral form,
protonated form and deprotonated form.

Figure SI-11. MOs involved in the three main electronic transition of neutral **1**.

Figure SI-12. MOs involved in the three main electronic transition of protonated **1**

Figure SI-13. VCD and IR of verdin **2** with added zinc triflate as function of time.

Figure SI-14. ECD and UV of verdins **1-6** in CHCl_3 solution with added zinc triflate.

Figure SI-15. ECD and UV of verdin **6** in 5×10^{-5} M CHCl_3 solution with added zinc chloride.

Figure SI-16. VCD, IR, ECD and UV spectra of 8,12-bis[(1*S*)-methylpropyl]mesobiliverdin-XIII α in chloroform with added zinc triflate.

Analysis of the dependence of the excitonic couplet molar intensity versus concentration and evaluation of association constant K_A .

Figure SI-17. Analysis of CD spectra of verdin **2** at different concentration.

Figure SI-18. Calculated ECD/UV and VCD/IR spectra for the dimer based on two M units.

Figure SI-19. Comparison between experimental and calculated IR spectra of zinc complexes of **2**.

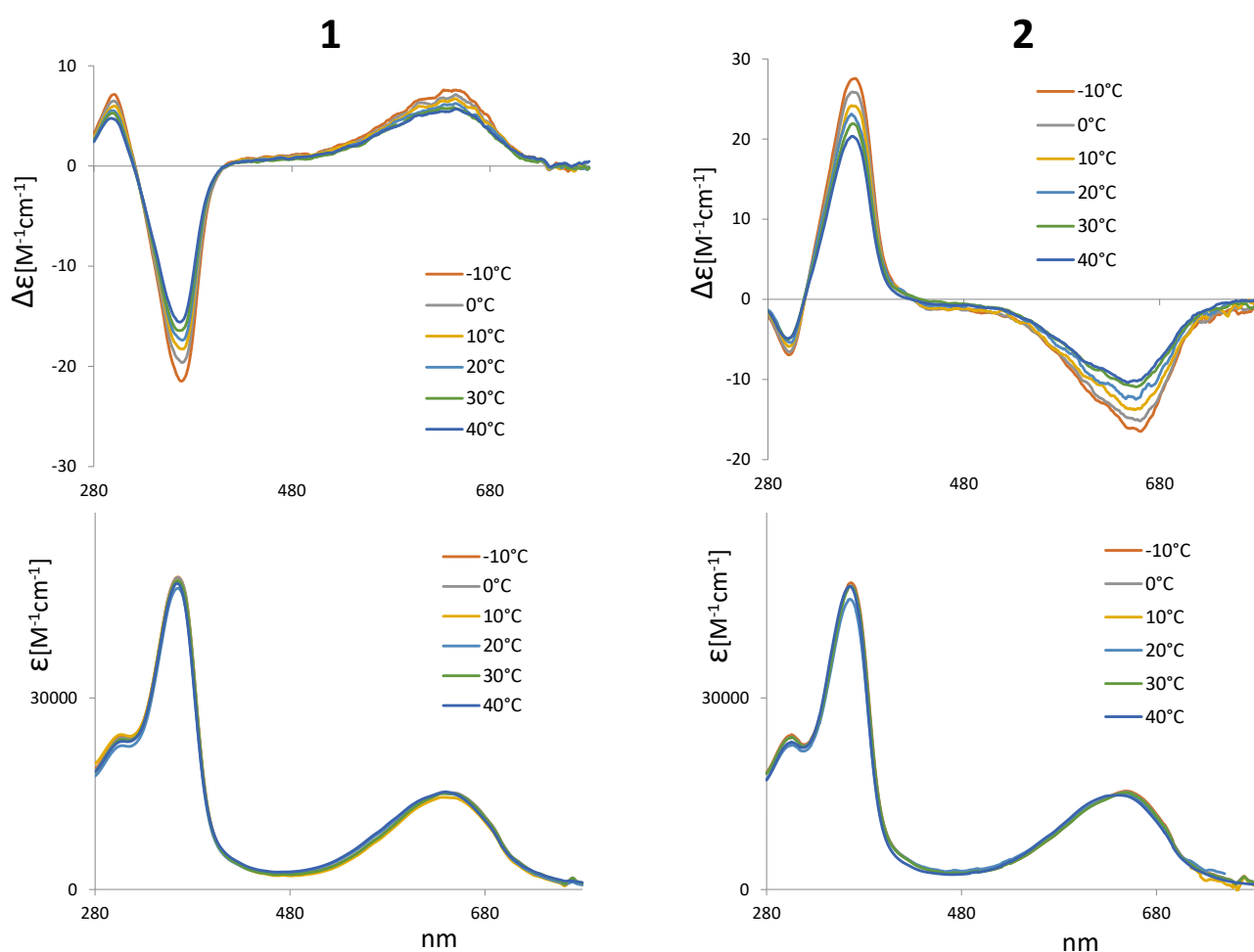


Figure SI-1. ECD and UV spectra of **1** (left) **2** (right) as a function of the temperature (from -10 °C to 40 °C).

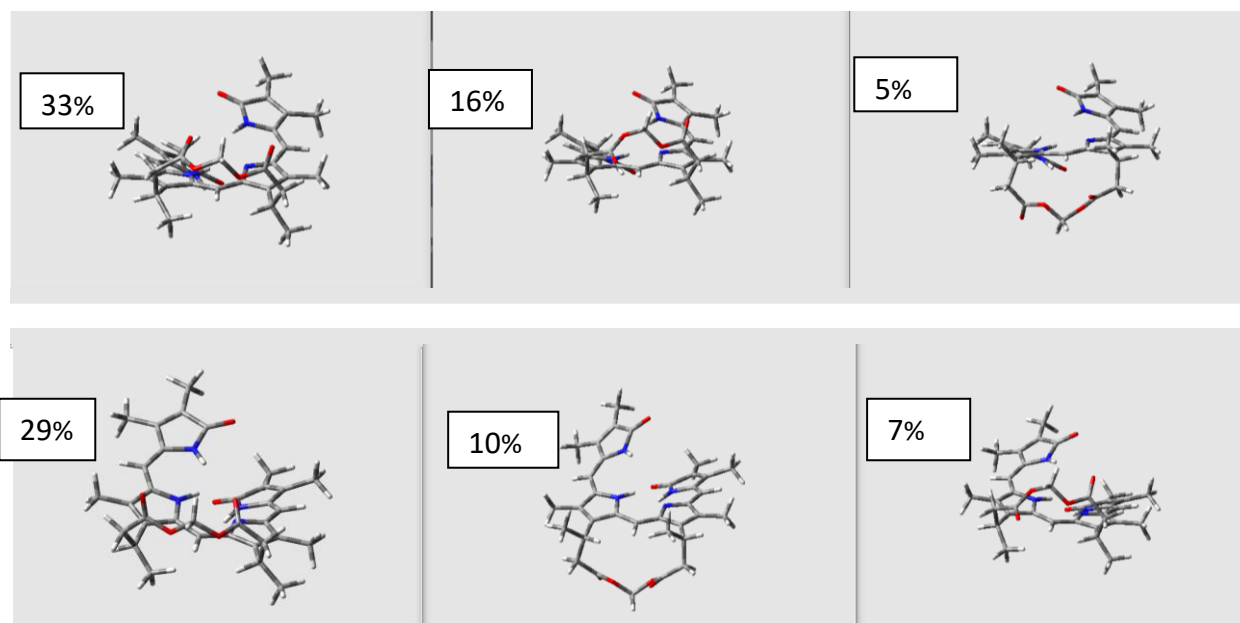


Figure SI-2. Optimized 3D-structures of the most populated conformers of **1** (DFT-B3LYP-TZVP). Top row: *P*-conformers, bottom row: *M*-conformers

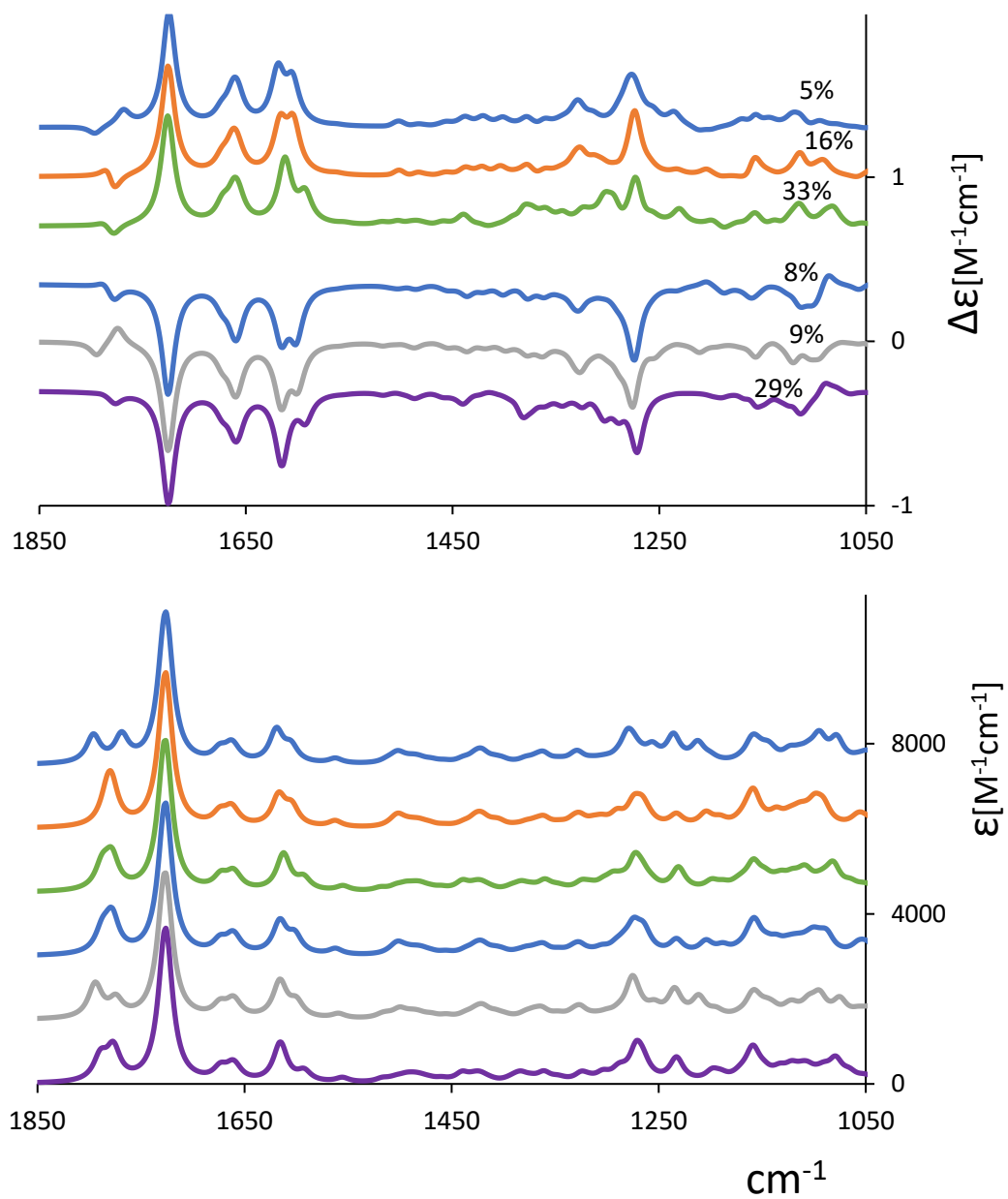


Figure SI-3. Calculated VCD (*top*) and IR (*bottom*) spectra of the most populated conformers of **1** (DFT-B3LYP-TZVP)

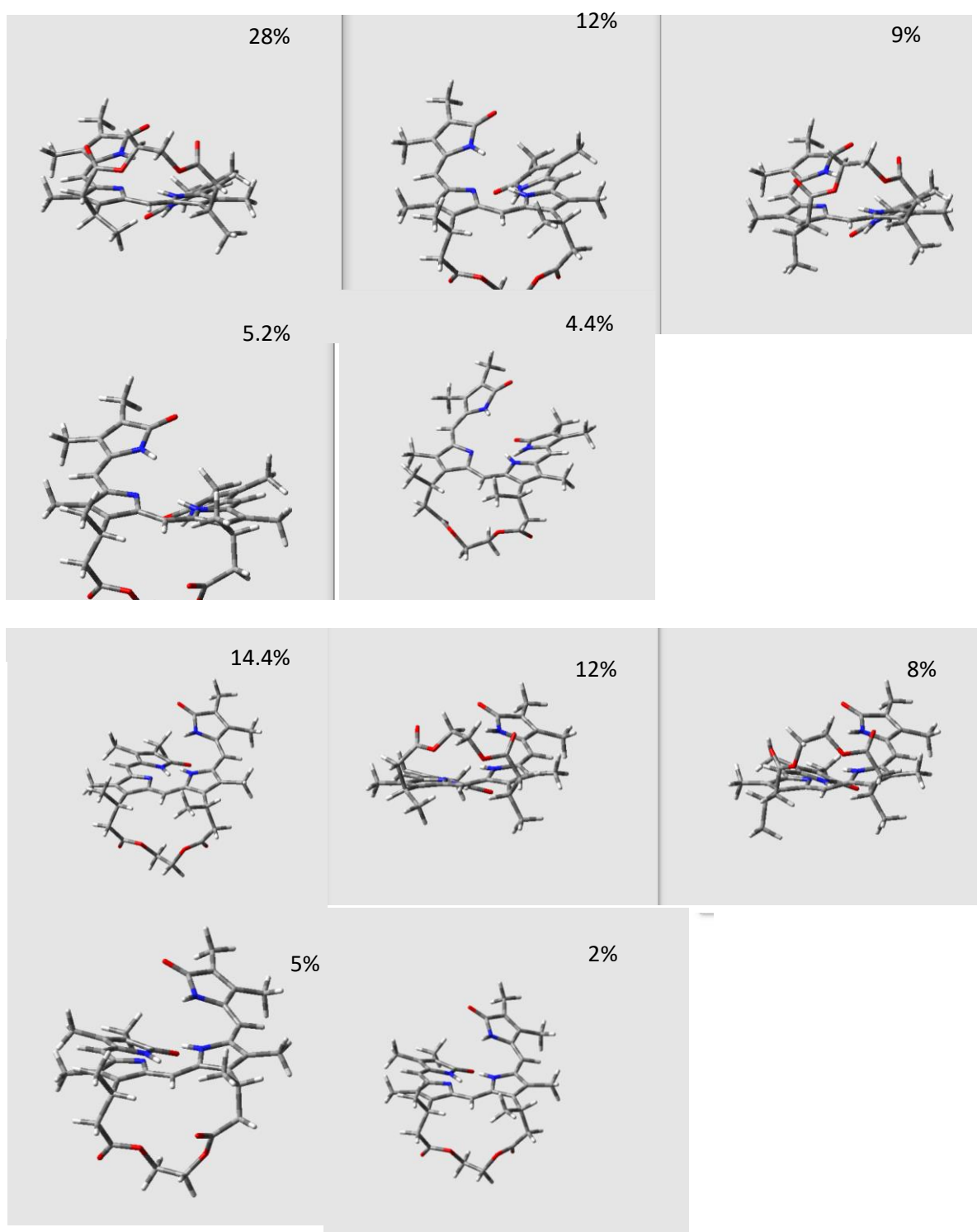


Figure SI-4. Optimized 3D-structures of the most populated conformers of **2** (DFT-B3LYP-TZVP). Top two rows: *M*-conformers, bottom two rows: *P*-conformers

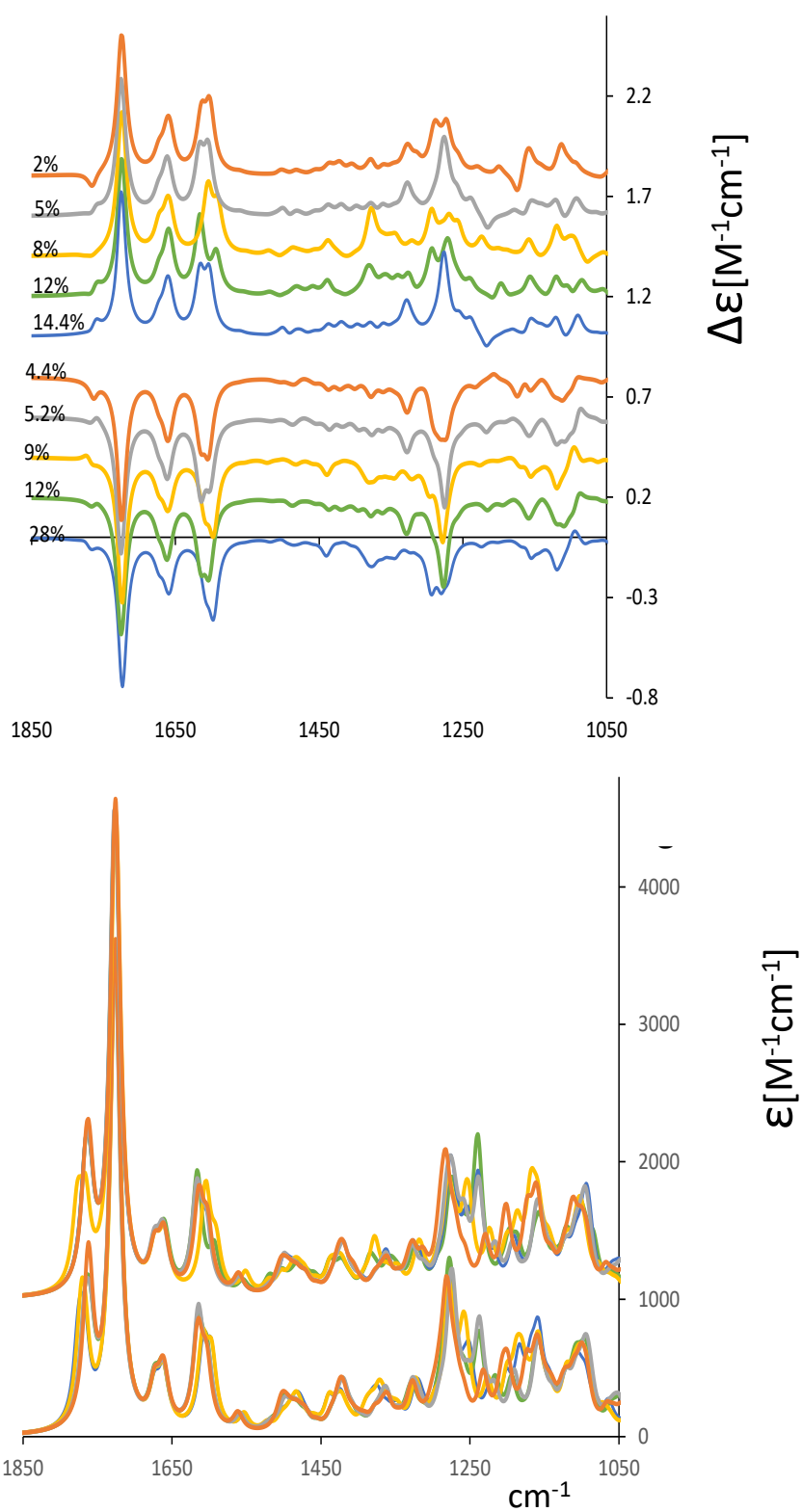


Figure SI-5. Calculated VCD (*top*) and IR (*bottom*) spectra of the most populated conformers of **2** (DFT-B3LYP-TZVP)

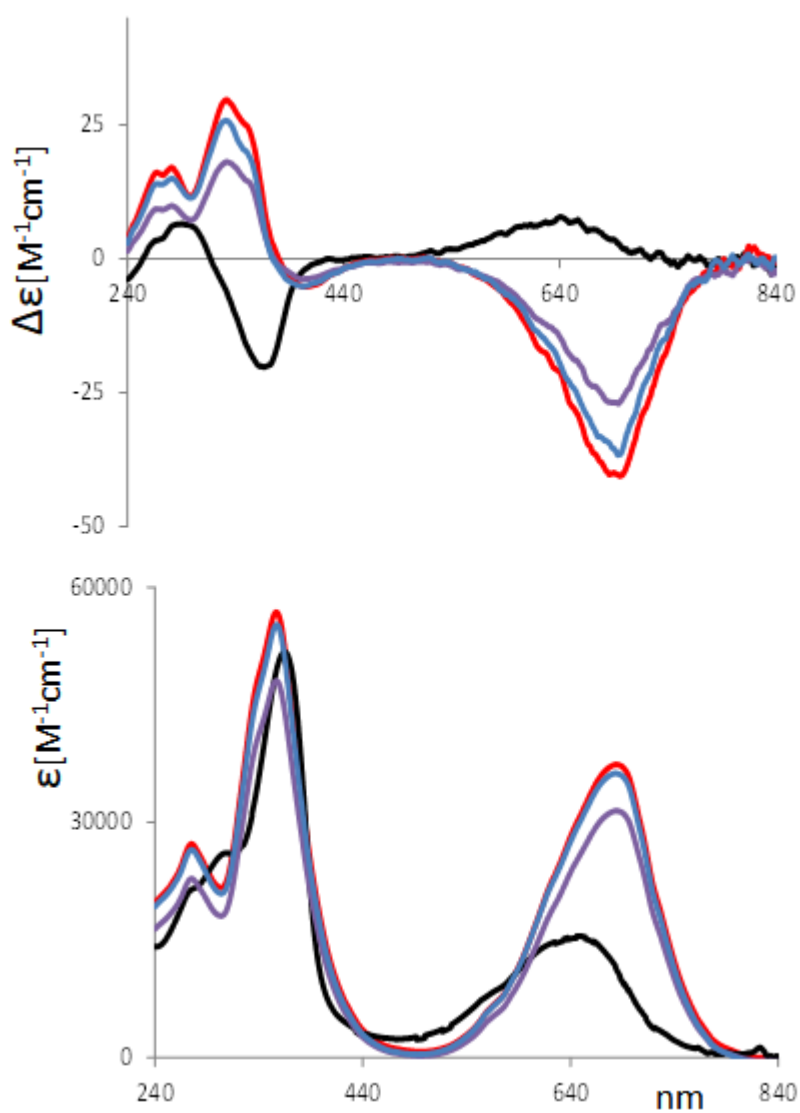


Figure SI-6. Experimental ECD (*top*) and UV (*bottom*) spectra of **1** in neutral 1×10^{-5} M methanol solution (black line) and after addition of HCl (from 0.004 M purple to 0.01 M red).

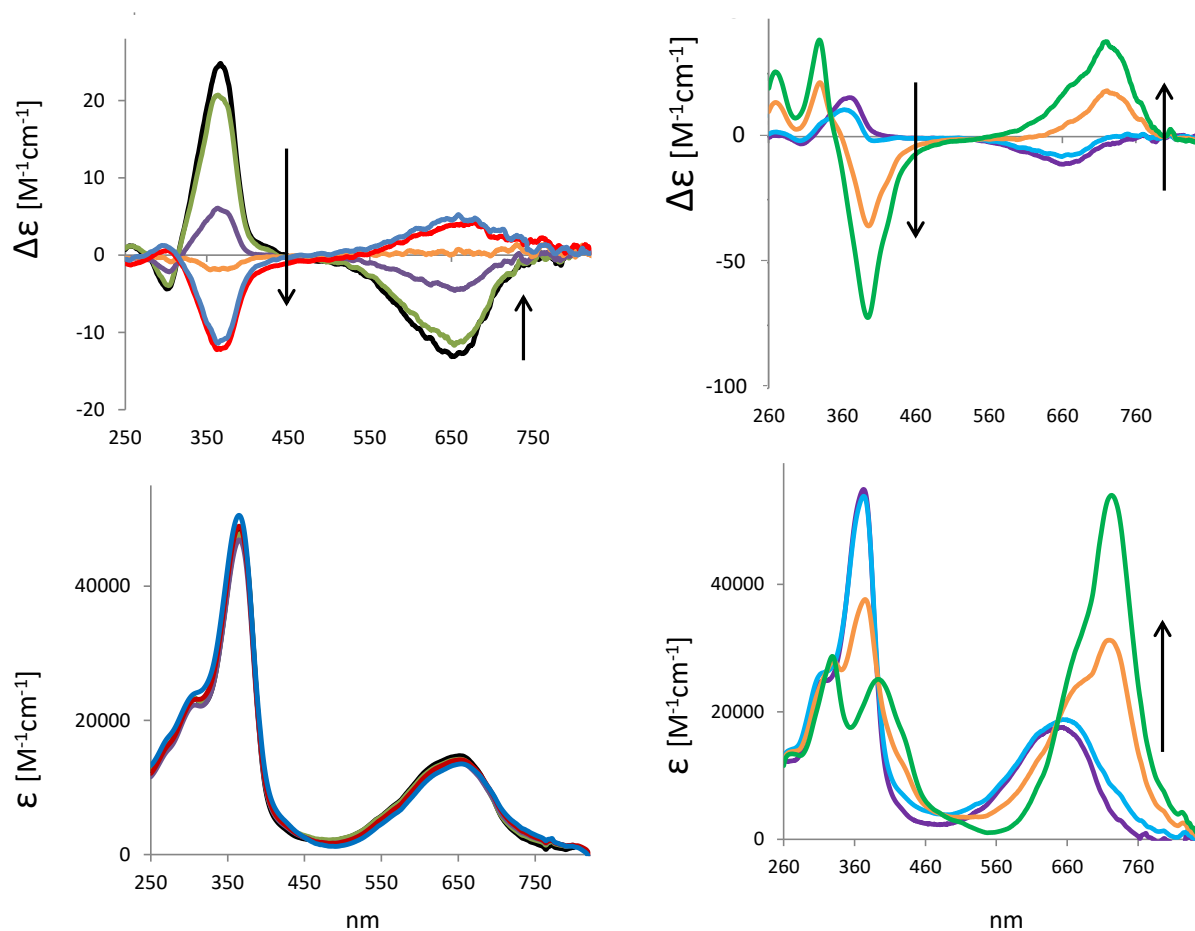


Figure SI-7. *Left:* Experimental ECD (*top*) and UV (*bottom*) spectra of **2** in neutral 1×10^{-5} M methanol solution (black line) and after addition of NaOH (from 0.002 M green to 0.01 M red). *Right:* Experimental ECD (*top*) and UV (*bottom*) spectra of **2** in neutral 1×10^{-5} M DMSO solution (purple) and after addition of NaOH (from 0.002 M light blue to 0.01 M green).

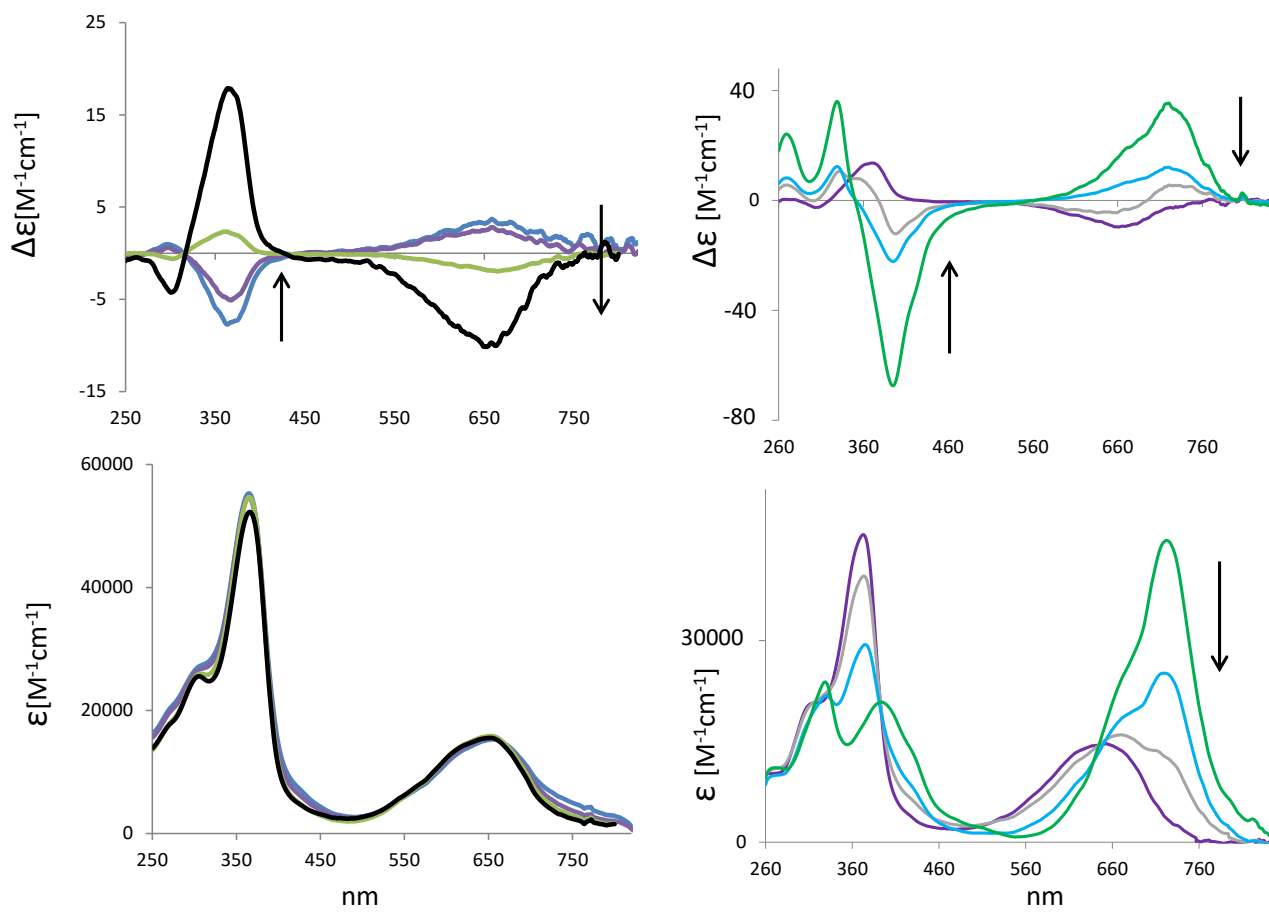


Figure SI-8. Experimental ECD (*top*) and UV (*bottom*) spectra of **2** during the neutralization in methanol (left) and DMSO (right). Starting from the basified condition (blue line for basic MeOH and green line for basic DMSO), HCl was added till the complete neutralization of the solution (black line for MeOH, purple line for DMSO).

Table SI-1. Boltzmann population factors for the six main conformers in the neutral and protonated condition for compound **1**.

conformer	Boltzmann pop% IEF-PCM MeOH	
	Neutral form	Protonated form
<i>1P</i>	32	19
<i>1M</i>	24	9
<i>2P</i>	18	21
<i>2M</i>	13	42
<i>3M</i>	11	7
<i>3P</i>	2	2
Sum <i>M-P</i>	<i>55P-45M</i>	<i>42P-58M</i>

Table SI-2. Boltzmann population factors for the ten main conformers in the neutral and deprotonated condition for compound **2**.

conformer	Boltzmann pop% IEF-PCM DMSO	
	Neutral form	Deprotonated form
<i>1M</i>	31	26
<i>1P</i>	18	29
<i>2M</i>	13	10
<i>2P</i>	12	17
<i>3M</i>	8	3
<i>3P</i>	6	5
<i>4P</i>	4	5
<i>4M</i>	4	2
<i>5M</i>	3	1
<i>5P</i>	1	2
Sum <i>M-P</i> pop%	<i>56M-44P</i>	<i>42M-58P</i>

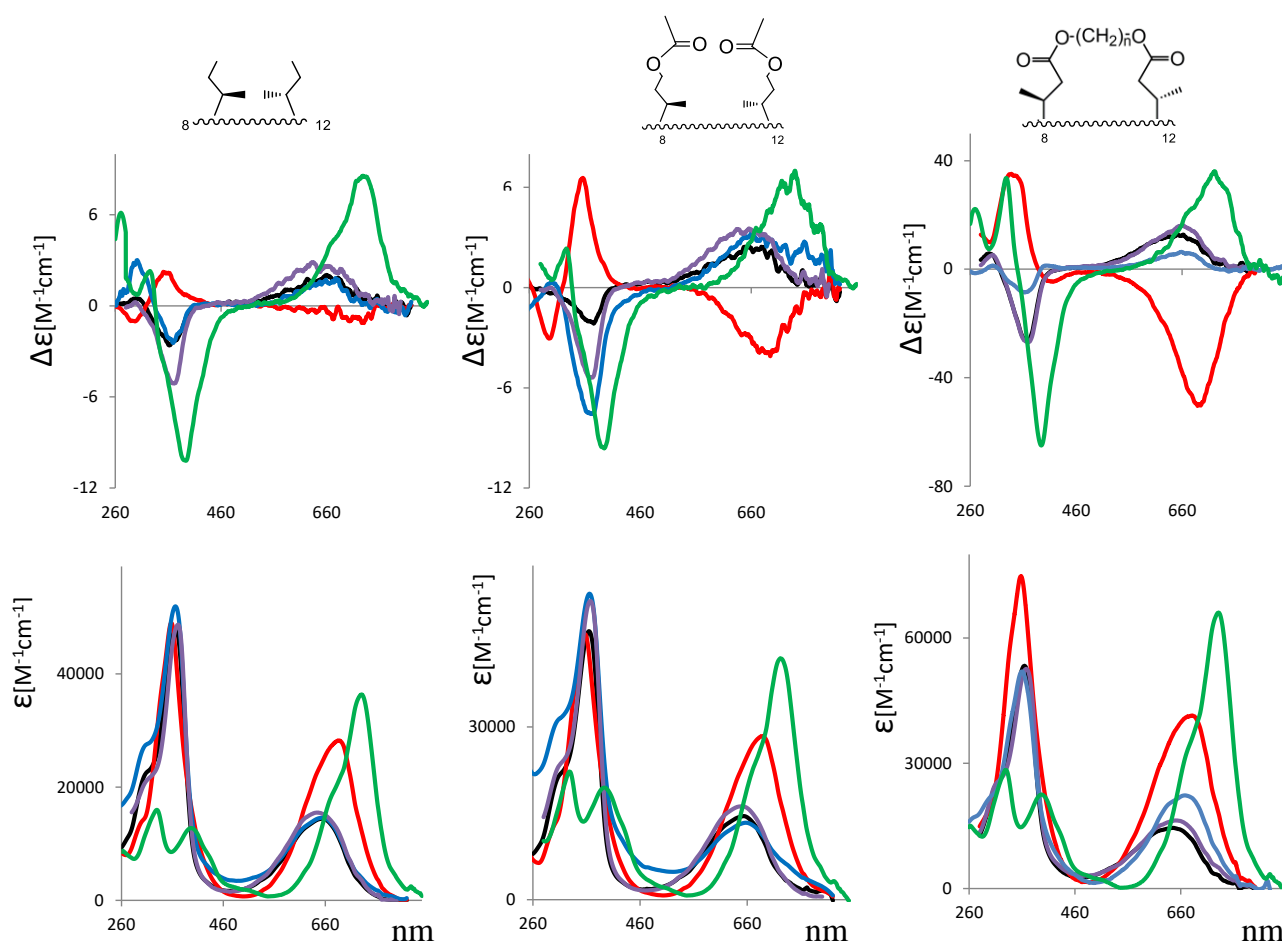


Figure SI-9. Experimental ECD (*top*) and UV (*bottom*) spectra of 8,12-bis[(1*S*)-methylpropyl]mesobiliverdin-XIIIa (*left*), 8,12-bis[3-acetoxy-(1*S*)-methylpropyl]mesobiliverdin-XIIIa (*center*), and **6** (*right*) in neutral 10^{-5} M methanol solution (black curves) and DMSO solution (purple curves), in the presence of 0.01 M of HCl (red curves) and in the presence of NaOH 0.02 M (blue curves for basified methanol and green curves for basified DMSO solutions, respectively).

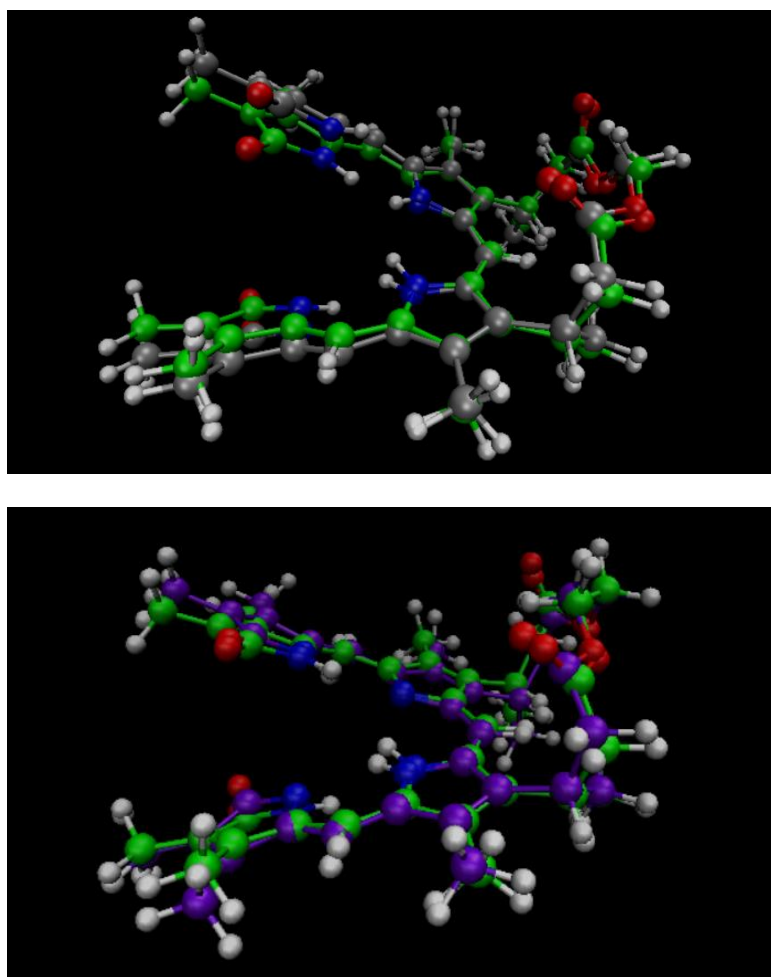


Figure SI-10. (*Top*) Superposed DFT-calculated structures for 1*P* conformer of **1** in the neutral form (green carbon atoms) and protonated form (grey carbon atoms). (*Bottom*) Superposed DFT-calculated structures for 1*P* conformer of **2** in the neutral form (green carbon atoms) and deprotonated form (purple carbon atoms).

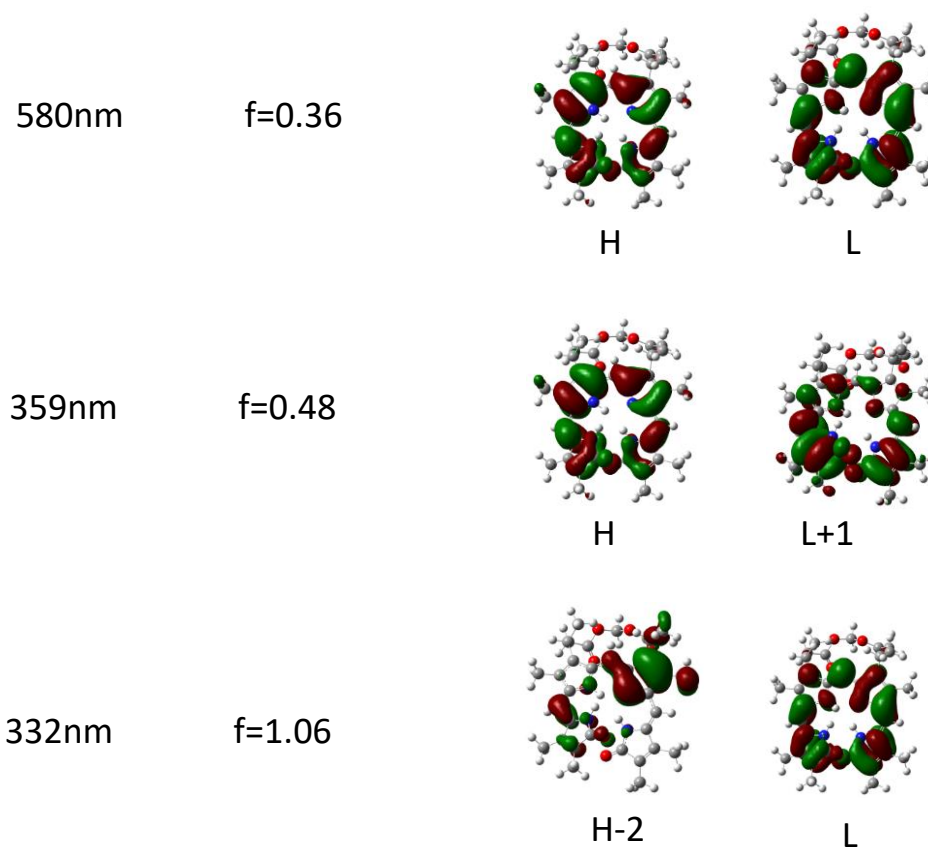


Figure SI-11. MOs involved in the three main electronic transition of neutral **1** (H stands for HOMO, L for LUMO). On the left wavelength and oscillator strength of the transition are given.

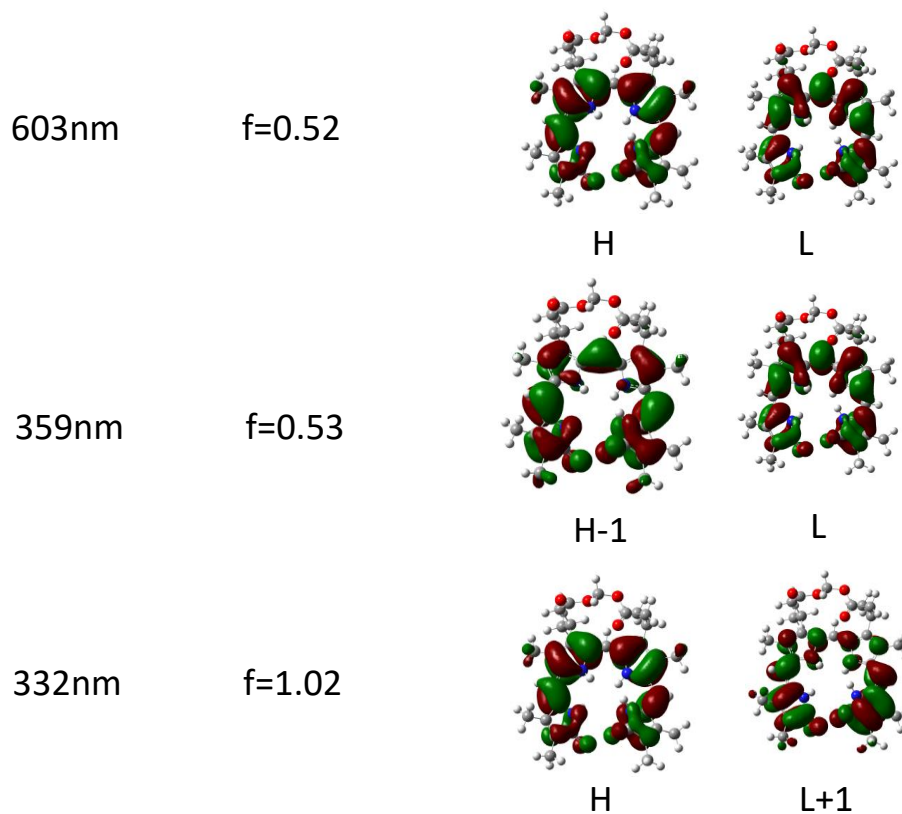


Figure SI-12. MOs involved in the three main electronic transition of protonated **1** (H stands for HOMO, L for LUMO). On the left wavelength and oscillator strength of the transition are given.

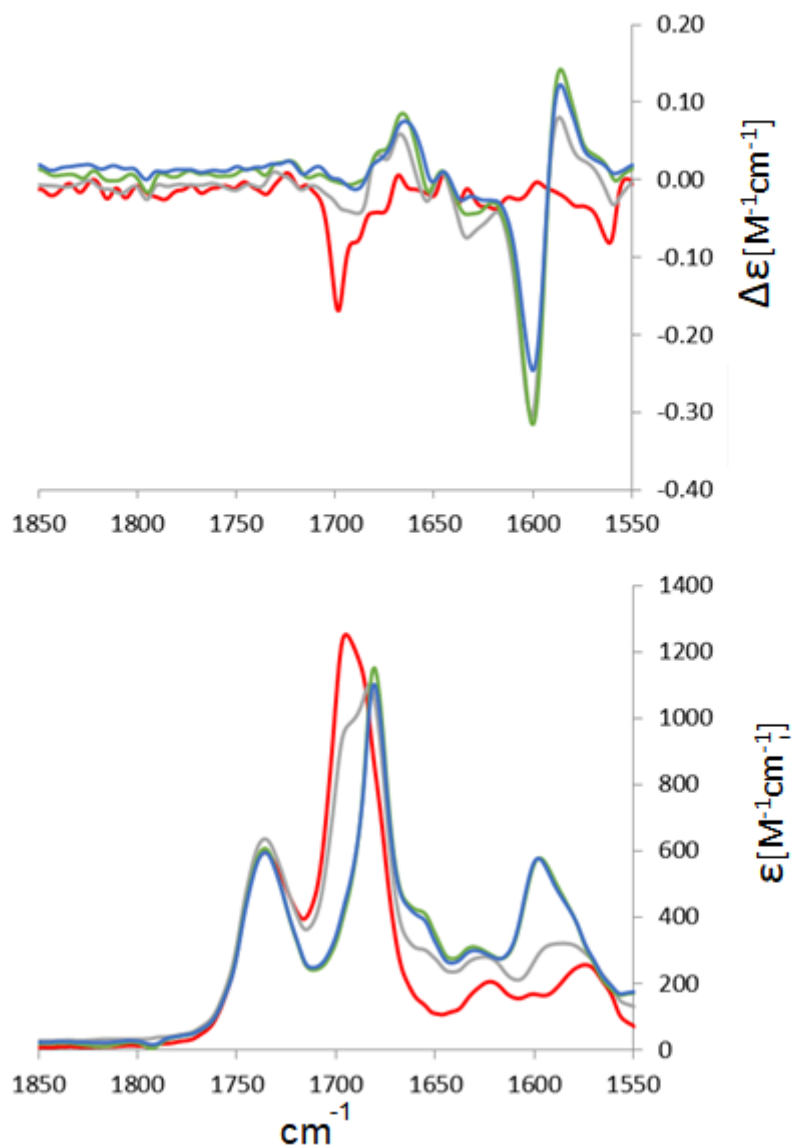


Figure SI-13. VCD (*top*) and IR (*bottom*) experimental spectra of verdin **2** in 10^{-3} M CDCl_3 solution in neutral form and with added zinc triflate. Red line: **2** neutral, grey: **2** + Zn triflate after 30 mins, blue: **2** + Zn triflate after 3 hours, green: **2** + Zn triflate after 5 hours .

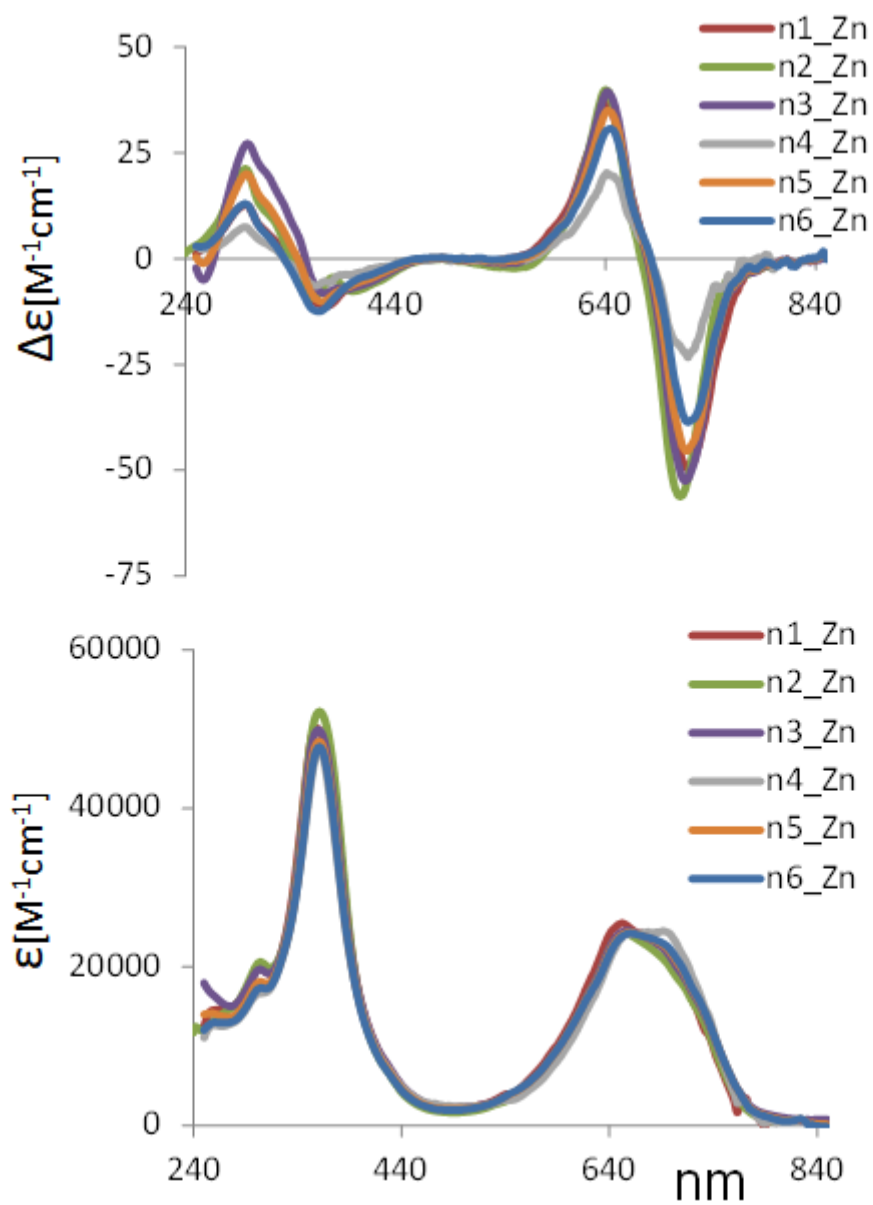


Figure SI-14. ECD (*top*) and UV (*bottom*) spectra of verdins **1-6** in 5×10^{-5} M $CHCl_3$ solution with added zinc triflate.

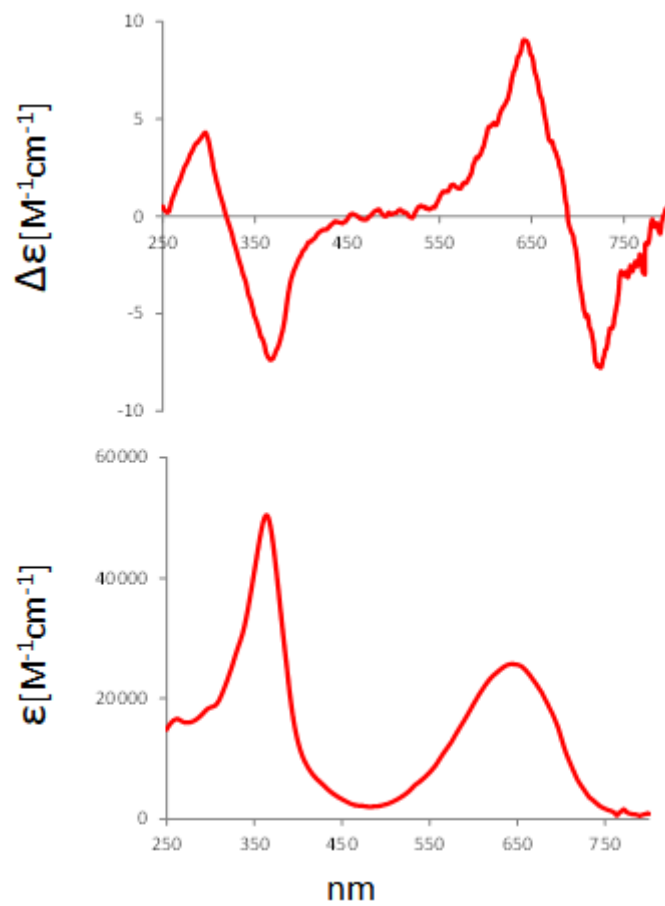


Figure SI-15. ECD (*top*) and UV (*bottom*) experimental spectra of verdin **6** in 5×10^{-5} M $CHCl_3$ solution with added zinc chloride.

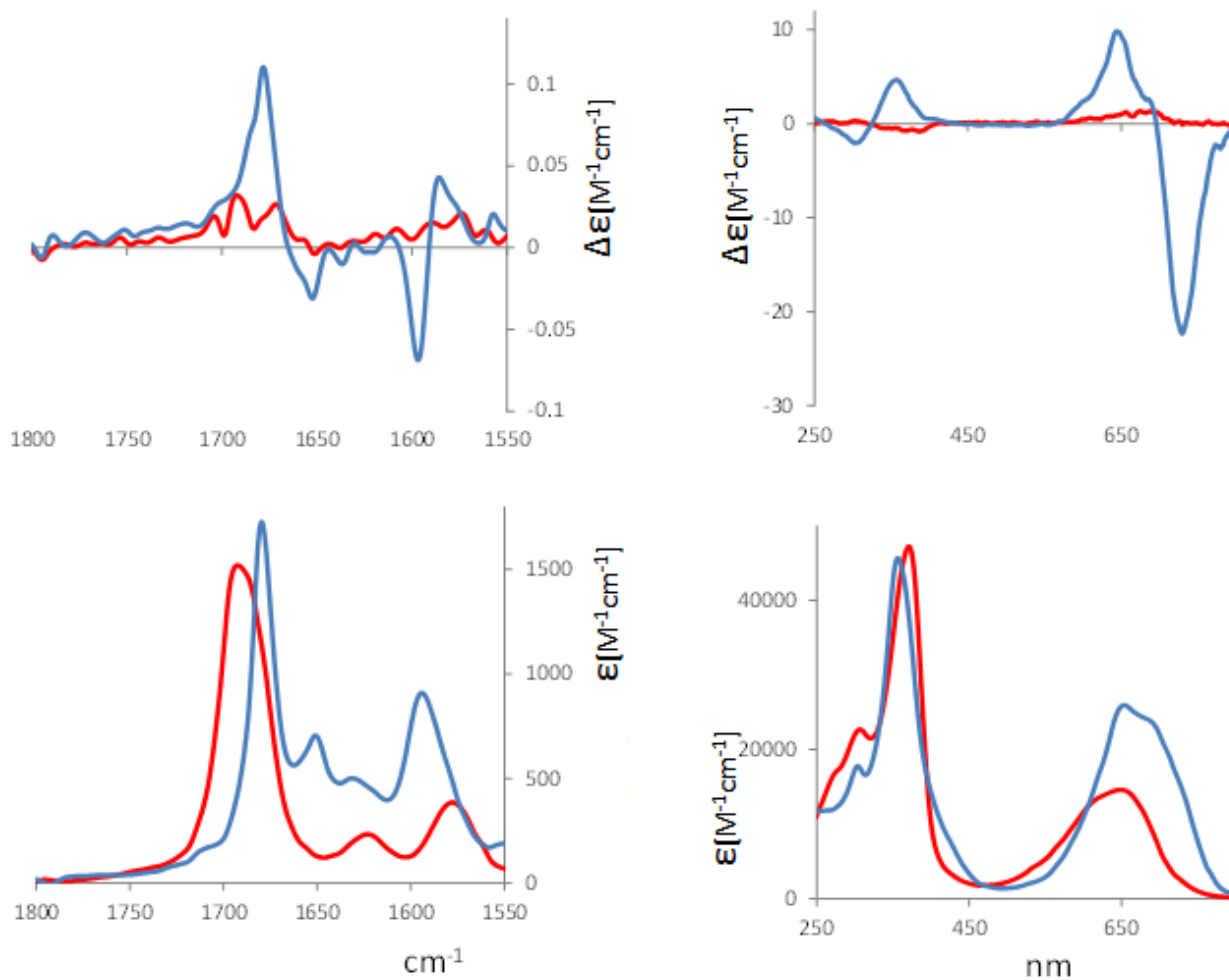


Figure SI-16. VCD, IR, ECD and UV spectra of 8,12-bis[(1*S*)-methylpropyl]mesobiliverdin-XIII α in chloroform (red line) and with added zinc triflate (blue line).

Analysis of the dependence of the excitonic couplet molar intensity versus concentration and evaluation of association constant K_A .

We treated the observed excitonic intensity values $\Delta\Delta\varepsilon_{obs} = \Delta\varepsilon_{max} - \Delta\varepsilon_{min}$ as function of concentration C_{tot} (reported in Figure SI-16A), analogously to what done in Nogales et al.[1] for chemical shift data signaling dimer formation. We assume that there are two species in solution and, due to the excitonic nature of the signal, we assume they are a monomeric species with vanishing $\Delta\Delta\varepsilon_M$, and a dimeric one with intrinsic $\Delta\Delta\varepsilon_D$ corresponding to the highest concentration spectrum.

We can write:

$$K_A = \frac{C_D}{C_M^2}; \quad \text{where} \quad C_{tot} = C_M + 2C_D; \quad (1)$$

where K_A is the association constant and C_{tot} is the concentration of the compound, which is partitioned in the concentration of the monomer C_M and of dimer C_D .

Assuming that $\Delta\Delta\varepsilon_{obs}$, is just due to $\Delta\Delta\varepsilon_D$ contribution, we may write:

$$\Delta\Delta\varepsilon_{obs} = \Delta\Delta\varepsilon_D \frac{2C_D}{C_{tot}} = \Delta\Delta\varepsilon_D \left(1 - \frac{C_M}{C_{tot}}\right) \quad (2)$$

and we obtain

$$C_M = \frac{(\Delta\Delta\varepsilon_D - \Delta\Delta\varepsilon_{obs})}{\Delta\Delta\varepsilon_D} C_{tot} \quad \text{and then} \quad K_A = \frac{\Delta\Delta\varepsilon_{obs} \Delta\Delta\varepsilon_D}{(\Delta\Delta\varepsilon_{obs} - \Delta\Delta\varepsilon_D)^2 2C_{tot}} \quad (3)$$

The last equation may be rewritten by taking the logarithm base e, as follows:

$$\log \Delta\Delta\varepsilon_{obs} - 2 \log(\Delta\Delta\varepsilon_D - \Delta\Delta\varepsilon_{obs}) = [\log K_A + \log 2 - \log \Delta\Delta\varepsilon_D] + \log C_{tot} \quad (4)$$

From Figure SI-16B one may verify that observed data are well represented by equation (4), with a linear dependence on $\log C_{tot}$, with coefficient 1. This observation is a strong backup to the proposed model for the monomer dimer equilibrium and permits us to evaluate the association constant $K_A = 72930 \text{ M}^{-1}$, assuming $\Delta\Delta\varepsilon_D = 158 \text{ M}^{-1}\text{cm}^{-1}$, the value recorded at the highest concentration.

As a further check, from equations (1), one may derive:

$$C_M = \frac{-1 + \sqrt{1 + 8K_A C_{tot}}}{4K_A} \cong \sqrt{\frac{C_{tot}}{2K_A}} \quad \text{in the limit of for } K_A C_{tot} \gg 1 \quad (5)$$

Considering equation (2) and (5), we obtain:

$$\Delta\Delta\varepsilon_{obs} \cong \Delta\Delta\varepsilon_D - \Delta\Delta\varepsilon_D (2K_A C_{tot})^{-1/2} \quad (6)$$

The last relation, used for data obtained on most concentrated solutions, permits us to check that the assumed $\Delta\Delta\varepsilon_D$ value is correct, as obtained from intercept of the equation of the straight line with the ordinate axis in Figure SI-16C and as shown in the equation within the same figure.

[1] Nogales. D. F.; Ma, J-S.; Lightner. D. A. Self-Association of Dipyrrinones Observed by 2D-NOE NMR and Dimerization Constants Calculated From $^1\text{H-NMR}$ Chemical Shifts. *Tetrahedron*, **1993**, *49*, 2361-2372.

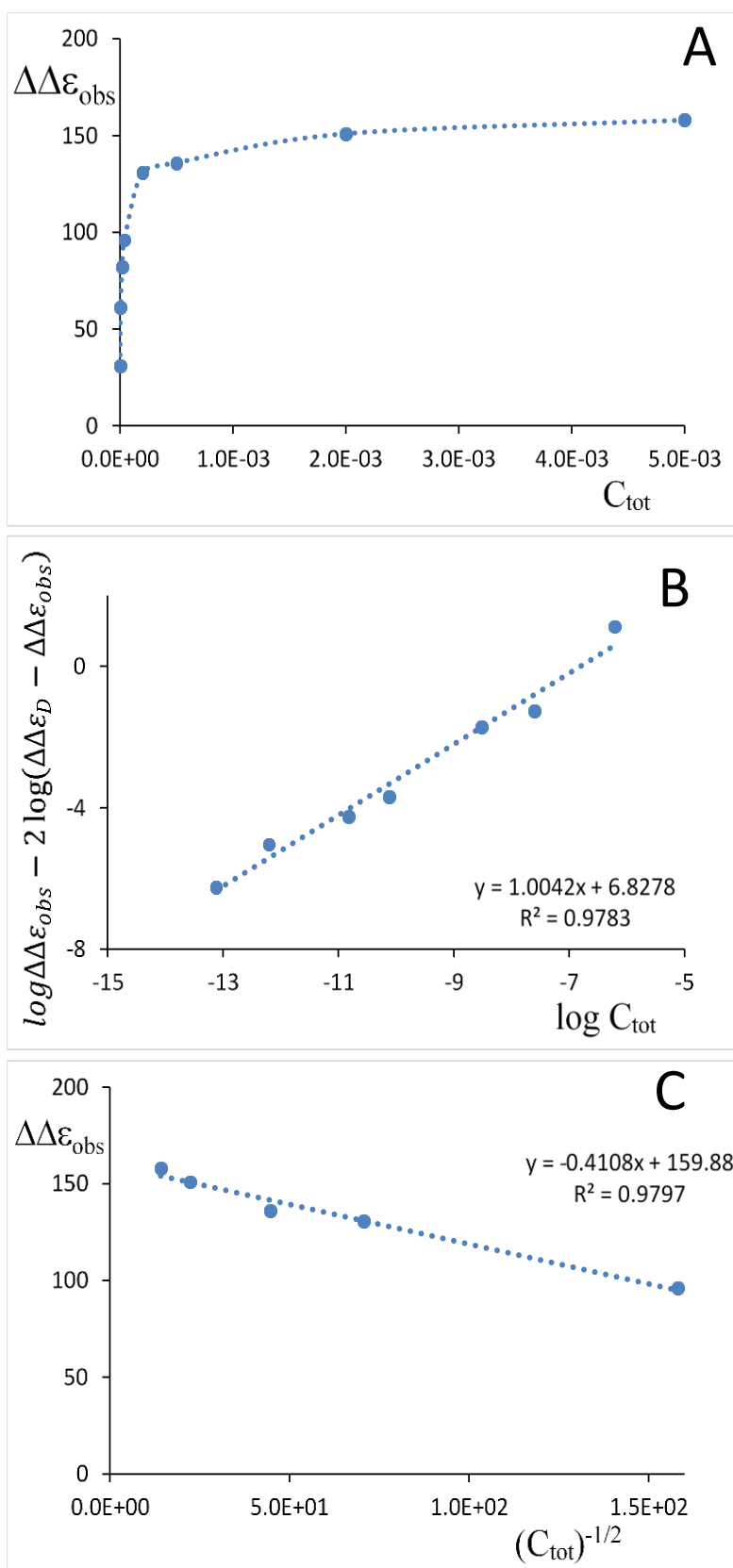


Figure SI-17. Analysis of CD spectra of verdin **2** at different concentration (Figure 7 in the text):
 A) Plot of excitonic intensity $\Delta\Delta\epsilon_{obs}$ vs concentration C_{tot}
 B) Plot of $\log\Delta\Delta\epsilon_{obs} - 2\log(\Delta\Delta\epsilon_D - \Delta\Delta\epsilon_{obs})$ versus $\log C_{tot}$ from which K_a has been deduced
 C) Plot of excitonic intensity $\Delta\Delta\epsilon_{obs}$ vs $(C_{tot})^{-1/2}$ for extrapolating $\Delta\Delta\epsilon_D$ concentration.

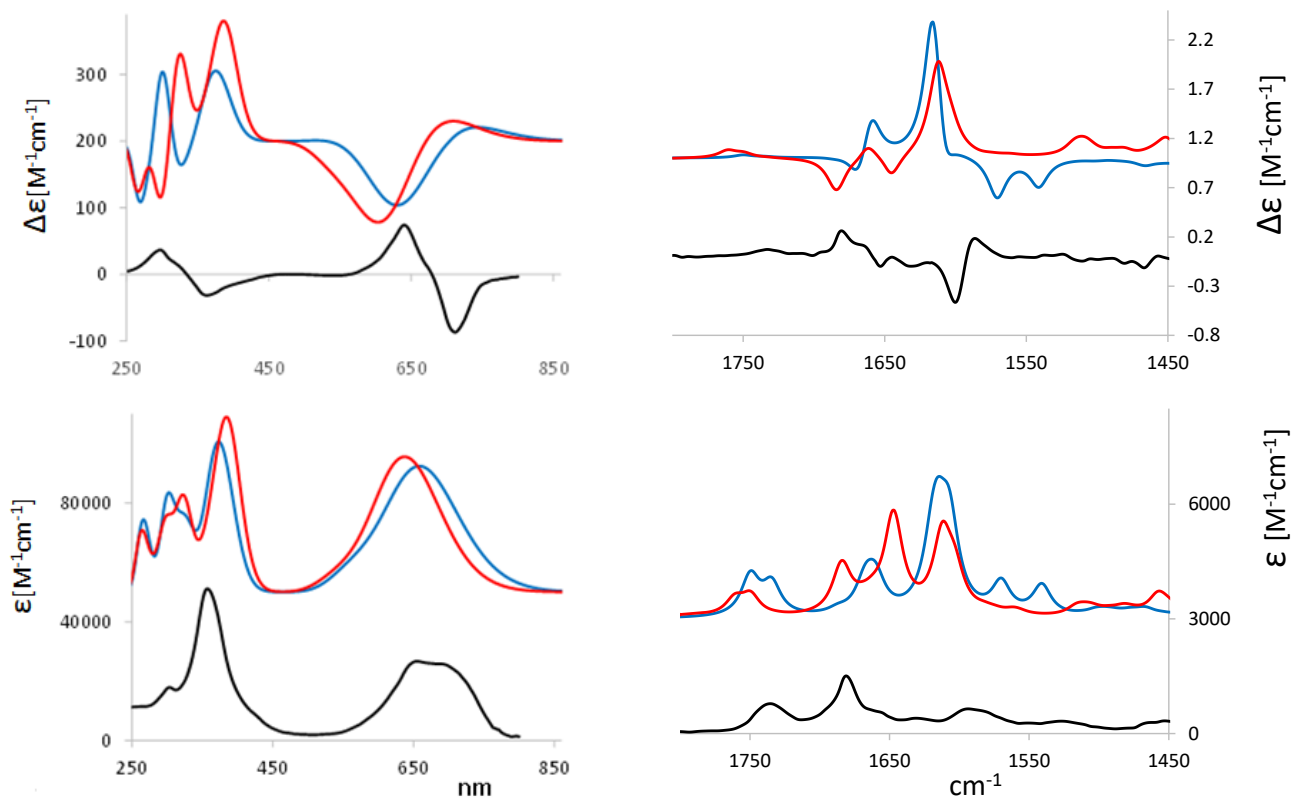


Figure SI-18. Comparison of experimental (black line) spectra of 10^{-3} M chloroform solution of Zn^{2+} -**2** with the calculated ECD/UV (left) and IR/VCD (right) spectra. Calculated spectra are shown for dianionic dimer (blue line), dimer lactam/lactim (red line) based on two M units.

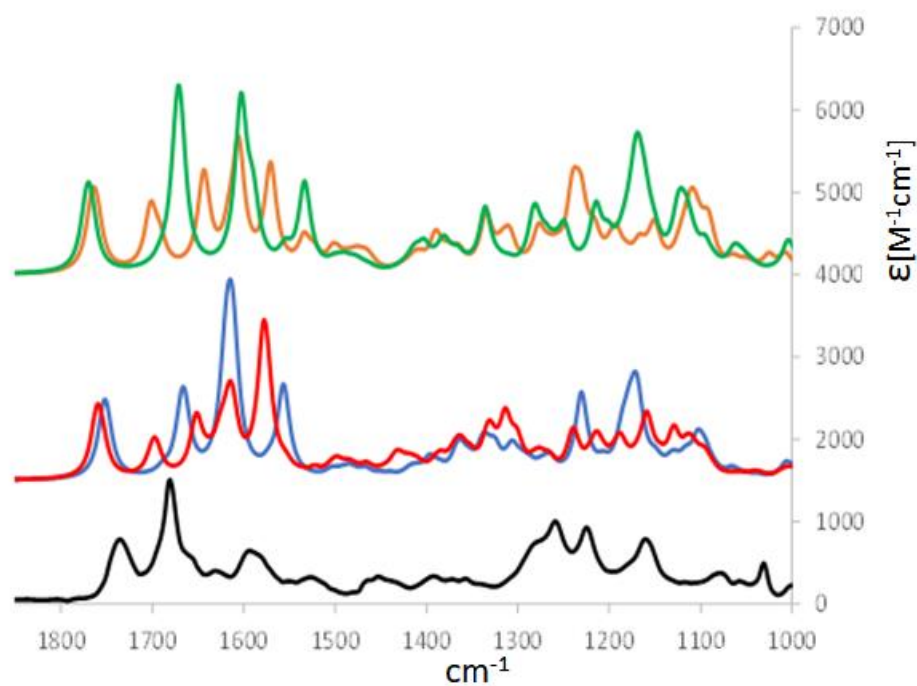


Figure SI-19. Comparison between experimental (black line) and calculated IR spectra of zinc complexes of **2**. Calculated IR are shown for dianionic dimer (blue line), dimer with a lactim ring for each biliverdin (red line), weighted average of anionic monomer (green line) and weighted average of lactam/lactim monomer (orange line).